doi:10.1016/j.jmb.2006.07.001 J. Mol. Biol. (2006) 362, 140–150

JMB

Available online at www.sciencedirect.com

ScienceDirect

ELSEVIER

Crystal Structure of Polymerization-Competent Actin

Vadim A. Klenchin[1], Sofia Y. Khaitlina[1,2] and Ivan Rayment[1]*

[1]*Department of Biochemistry University of Wisconsin Madison, WI 53706, USA*

[2]*Department of Cell Culture Institute of Cytology Russian Academy of Sciences Tykhoretsky Avenue, 4, 194064 St. Petersburg, Russia*

**Corresponding author*

All actin crystal structures reported to date represent actin complexed or chemically modified with molecules that prevent its polymerization. Actin cleaved with ECP32 protease at a single site between Gly42 and Val43 is virtually non-polymerizable in the Ca-ATP bound form but remains polymerization-competent in the Mg-bound form. Here, a crystal structure of the true uncomplexed ECP32-cleaved actin (ECP-actin) solved to 1.9 Å resolution is reported. In contrast to the much more open conformation of the ECP-actin's nucleotide binding cleft in solution, the crystal structure of uncomplexed ECP-actin contains actin in a typical closed conformation similar to the complexed actin structures. This unambiguously demonstrates that the overall structure of monomeric actin is not significantly affected by a multitude of actin-binding proteins and toxins. The invariance of actin crystal structures suggests that the salt and precipitants necessary for crystallization stabilize actin in only one of its possible conformations. The asymmetric unit cell contains a new type of antiparallel actin dimer that may correspond to the "lower dimer" implicated in F-actin nucleation and branching. In addition, symmetry-related actin-actin contacts form a head to tail dimer that is strikingly similar to the longitudinal dimer predicted by the Holmes F-actin model, including a rotation of the monomers relative to each other not observed previously in actin crystal structures.

Keywords: actin polymerization; ECP32 protease; crystal structure; G-actin; F-actin

Introduction

The unique physiological role of actin as a structural component of the cytoskeleton and a regulator of numerous cellular processes relies in large part on the existence of a dynamic equilibrium between monomeric G-actin and polymeric F-actin forms.[1] Actin filament dynamics is tightly coupled to the high conformational flexibility exhibited by the protein. A full understanding of actin-mediated cellular processes, therefore, requires a structural description of its conformational changes at high resolution.

Actin belongs to a superfamily of ATPases that includes the ATP-binding domain of the Hsp70-related proteins, sugar kinases, actin-related proteins and prokaryotic actin homologs that, despite their lack of amino acid sequence similarity, share a common fold.[2–4] The common core architecture consists of two large domains connected by a hinge and a nucleotide binding site located in the cleft between the domains. The largest conformational change observed or proposed for this class of proteins is associated with a transition between the open and closed nucleotide binding cleft to allow nucleotide exchange. For example, hexokinase requires such a conformational change as a part of its catalytic mechanism[5,6] and the essential cleft opening in the Hsp70-related proteins is regulated by binding of nucleotide exchange factors.[7,8] Similar conformational changes have been suggested to occur in G-actin[9,10] and F-actin.[11,12] Actin conformational changes consistent with an equilibrium between closed and open states of the nucleotide binding cleft have been observed by numerous approaches: kinetics of nucleotide exchange,[13,14] actin sensitivity to limited proteolysis,[15,16] synchrotron X-ray radiolysis[17,18] and electron microscopy reconstructions of F-actin filaments.[19–21] Additionally, a recent neutron scattering study suggests a dramatic structural change from a spherical G-actin form to an oblate ellipsoid in F-actin.[22]

In contrast to the biochemical studies that imply a high level of structural plasticity, actin crystal

Abbreviation used: ECP-actin, protease ECP32-cleaved actin.

E-mail address of the corresponding author: ivan_rayment@biochem.wisc.edu

structures available to date paint a different picture. All but one of them found actin in a conformation with the nucleotide binding cleft closed.[23–36] While the open state has been observed in a particular crystal form of profilin-bound actin crystals,[37] the relevance of this structure to the putative open conformation in solution has been questioned.[38,39] Two conflicting views have been expressed regarding the biochemical identity of the open and closed conformations. In one proposal, the open and closed conformations are identified as the ADP- and ATP-bound forms, respectively.[19,21] The other view is that any nucleotide-bound form of actin exists in the closed conformation and the open conformation represents nucleotide-free form.[28,38] In addition to the open conformation in actin-profilin crystals, another significant conformational change detected in actin crystal structures is a loop to helix transition of a part of actin subdomain 2 observed in tetramethyl-rhodamine-modified ADP- but not ATP-actin.[25,38]

In order to be crystallized, actin must be rendered non-polymerizable and, thus, all actin crystal structures available to date represent *complexes* of actin with actin binding proteins,[23,24,27,29,31] organic toxins[26,30,32–36] or with the covalently bound large hydrophobic probe, tetramethyl-rhodamine.[25,28] All of these binding partners (with the exception of profilin) impart a more closed conformation on actin as judged by their inhibition of nucleotide exchange.[14,40–42] Therefore, it is possible that the structures of actin complexes do not faithfully reflect the true structure of an uncomplexed form. A crystal structure of uncomplexed actin would seem to be the only direct way of resolving this uncertainty.

An abundance of X-ray structures of monomeric actin are now available but the structure of its polymeric F-actin form remains unknown.[43] Although F-actin was successfully modeled at low resolution based on actin fiber diffraction,[11,12,43,44] it is still unknown how the crystal structures of actin obtained are related to the conformation within actin filaments and the nature of actin-actin contacts at high resolution has yet to be established.

Actin can be specifically cleaved by a bacterial ECP32 protease at a single site between Gly42 and Val43 within the DNase-binding loop[45,46] (Figure 1). The ECP32-cleaved actin (ECP-actin) retains many features of the intact protein, including its ability to polymerize in the Mg-ATP bound form[47] or in the presence of myosin S1 fragment.[48] In the Ca-ATP bound form, however, it is virtually non-polymerizable.[45,47] Importantly, unlike the complexed actin species that have equilibrium shifted toward a more closed conformation of the nucleotide binding cleft, the ECP-actin in both G-and F-actin forms is clearly in a more open conformation as evidenced by the increased nucleotide exchange rate and its higher susceptibility to limited proteolysis.[15,49] Since ECP-actin is the only polymerization-competent actin that crystallizes without a binding partner, its seems to be an ideal candidate for X-ray diffraction structural studies. This work describes the crystal structure of ECP-actin solved at 1.9 Å resolution.

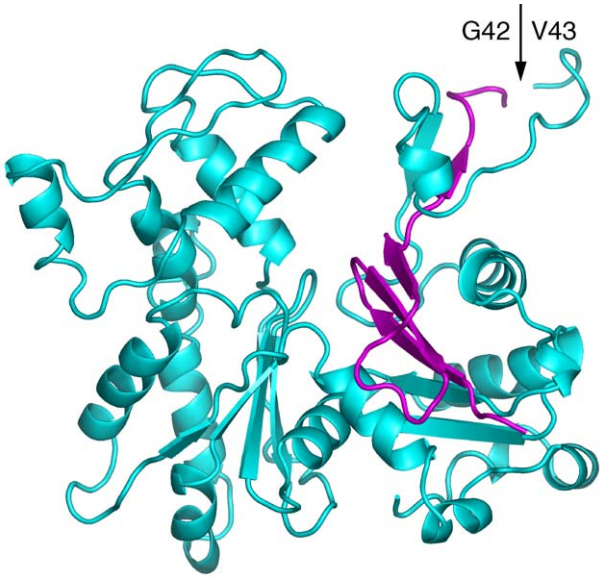

Figure 1. Actin cleavage by ECP32 protease. Shown is a ribbon diagram of a typical actin monomer and the location of a proteolytic cleavage site between Gly42 and Val43. The resulting two fragments (shown in cyan and magenta) remain associated such that the ECP-actin retains most of the features of the intact protein, including its ability to polymerize in the Mg-ATP bound form.

Results and Discussion

Crystal growth and structure determination

ECP-actin crystallized only in the presence of 20-50 mM $CaCl_2$ or $SrCl_2$. This corresponds to a salt concentration that is sufficient to induce polymerization of native actin. It has been previously been shown that the critical concentration for the KCl-induced polymerization of Ca^{2+}-bound ECP-actin containing Ca^{2+} was greater than 72 μM but decreased to 2.7 μM after replacement of the tightly bound Ca^{2+} with Mg^{2+}.[47] Consistent with these observations, 100 μM ECP-actin placed into crystallization-like conditions formed filamentous structures when the buffer contained 40 mM $MgCl_2$ but not $CaCl_2$ or $SrCl_2$. Importantly, Ca^{2+}-ECP-actin can still polymerize provided that its concentration is high enough. Approximately 30% of Ca^{2+}-ECP-actin at 330 μM could be pelleted in the presence of KCl, indicating that it remains polymerization-competent even in the absence of Mg^{2+}. This argues that ECP-actin can undergo salt-dependent conformational changes inherent of the native protein and that its crystal structure has the potential to reflect the structure of the protomer within actin filament.

Several factors proved to be critical for obtaining diffraction quality crystals of ECP-actin. First,

Table 1. Data collection and refinement statistics

Data collection	
Space group	$P2_12_12_1$
Unit cell dimensions	
a (Å)	63.9
b (Å)	198.1
c (Å)	69.6
Resolution (Å)	30–1.9
Observed reflections	1,150,388
Unique reflections	70,540
Redundancy	16.3 (14.4)
Average I/σ	43.3 (7.7)
Completeness (%)	99.9 (99.7)
R_{merge} (%)	7.3 (48.4)
Refinement	
Number of atoms	
Protein	5732
Sr-ATP	64
Solvent	696
R_{work} (%)	17.8 (19.8)
R_{free} (%)	21.5 (26.5)
Average B-factors (Å^2)	
Protein	22.8
Sr^{2+}-ATP	16.2
Solvent	35.1
r.m.s. deviations	
Bond angles (deg.)	1.277
Bond lengths (Å)	0.011
Ramachandran plot (%)	
Most favored	95
Additional allowed	5

Values in parentheses are for the outer resolution shell.

nucleation of crystal growth is clearly the most limiting step. The diffracting crystal form was originally obtained by epitaxial nucleation from crystals of ECP-actin-jaspisamide A complex[30] and all subsequent crystal growth was crucially dependent on seeding crystallization samples with microcrystals. Crystals form in the presence of ATP but not ADP. This is probably due to the intrinsic instability of ECP-actin complexed with ADP. The presence of high concentrations of divalent ions, Ca^{2+} or Sr^{2+} was absolutely essential. No crystal growth was observed in the presence of Mg^{2+}, presumably because of polymerization of Mg^{2+}-ECP-actin.[47] ECP-actin crystals are unstable and dissolve spontaneously within a few days at room temperature and within one-two weeks in the cold room. The addition of ethylene glycol partially protected the crystals against this deterioration, allowing the growth of larger and better diffracting crystals.

ECP-actin crystals grown in the presence of $CaCl_2$ or $SrCl_2$ both belong to the space group $P2_12_12_1$ with unit cell dimensions of $a=63.9$ Å, $b=198.3$ Å, $c=69.6$ Å and contain two actin molecules in the asymmetric unit. Crystals diffracted better when grown in the presence of Sr^{2+} and were used to collect data. The structure was solved to a 1.9 Å resolution by molecular replacement. Crystallographic statistics are presented in Table 1.

Overview of the ECP-actin structure

The asymmetric unit of ECP-actin crystals contains an antiparallel actin dimer (Figure 2(a)). As observed for other crystal structures of ATP-bound actin,[26–36] electron density is not present for the most flexible region of the subdomain 2, residues ~40-50. Molecules related by non-crystallographic symmetry can be superposed with a r.m.s. deviation of 0.66 Å over all Cα atoms. As outlined below, most of the difference is accounted for by movements of

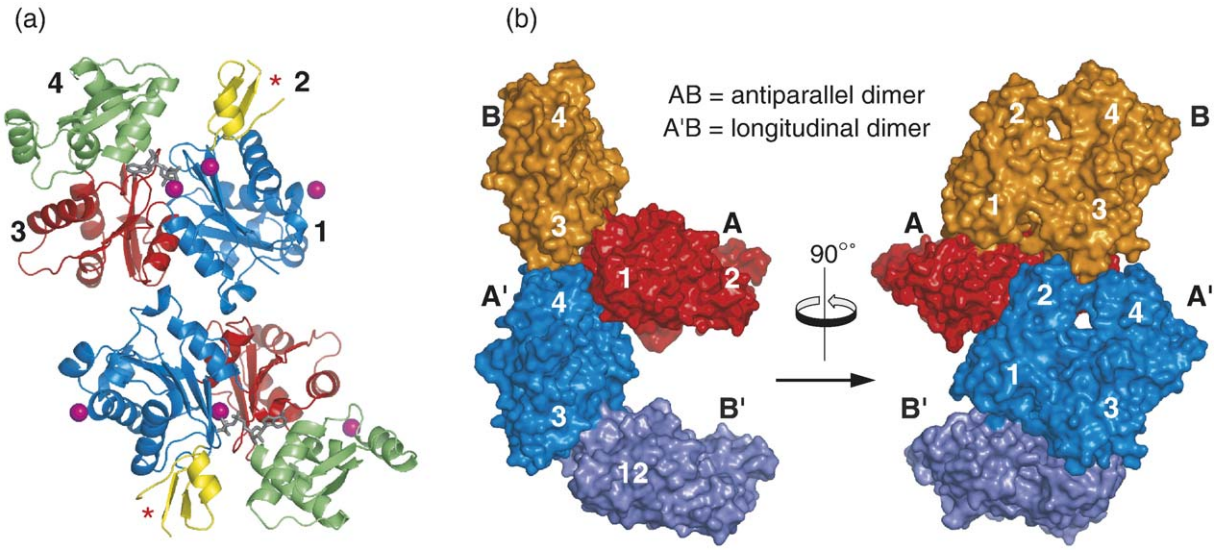

Figure 2. Asymmetric unit cell and crystal lattice contacts in ECP-actin crystals. (a) Antiparallel actin dimer found in the asymmetric unit cell. Actin subdomains one through four are color coded and labeled. Electron density is not present for residues 40-50 (positions are labeled as asterisks). The structures of monomers within the dimer differ somewhat due to the different crystal lattice contacts (see Figure 3). Strontium ions identified in the structure are shown in magenta spacefill representation. One additional strontium ion complexed by symmetry-related molecules is not shown. (b) Interaction of the symmetry related antiparallel dimers (AB, orange and red, and A'B', blue and violet) results in a formation of F-actin like longitudinal dimer (A'B, orange and blue).

flexible loops at points where crystal lattice contacts differ.

The antiparallel ECP-actin dimer is distinct from a disulfide bridged antiparallel actin dimer observed previously[26,32] – the distance between sulfur atoms in the opposing Cys374 residues is 29 Å and the orientation of the monomers is completely different. The most prominent contact between symmetry-related antiparallel dimers in the ECP-actin crystal lattice is shown in Figure 2(b). It illustrates that the interaction of the two antiparallel dimers (AB and A′B′) forms a new, parallel, actin dimer (A′B) that is stabilized by a third actin molecule (A) bound to both of the subunits of the dimer. This head to tail dimer is very similar to the longitudinal actin dimer predicted by the Holmes F-actin model and its actin-actin interface is discussed in detail below. The antiparallel actin dimer (the so called "lower dimer") has been shown to be an early product of actin polymerization that can nucleate filament growth and can incorporate into growing actin filaments yielding initially ragged and branched F-actin.[50] Based on this and similar observations, a model for an antiparallel actin dimer as an intermediate in the F-actin nucleation and filament branching has been proposed.[32,51] The antiparallel dimer of the type observed in ECP-actin crystals is compatible with this hypothesis. Figure 2(b) shows how it can incorporate into filaments and how the interaction of actin monomer with the antiparallel dimer can nucleate filament growth by forming a trimer (ABA′) in which one of the actins (A) effectively serves as a F-actin side-binding protein. The extensive hydrophobic and hydrogen bonding interactions at the interface, combined with the relatively large total surface area buried upon formation of this putative trimer, 2639 Å^2, suggests that such a trimer may be sufficiently stable to be a physiologically relevant and effective polymerization nucleus. On the other hand, the disulfide-stabilized antiparallel dimer previously proposed for this role,[26,32] seems a less likely candidate due to the significant reducing potential of the cytoplasm.

Overall, the structure observed for the ECP-actin monomer is surprisingly similar to the structures of native actin complexed with molecules that inhibit polymerization. ECP-actin is found in the typical closed conformation of the nucleotide binding cleft. If not for the *a priori* knowledge that the crystallized ECP-actin consists of two non-covalently linked polypeptide chains, nothing in the solved structure would point to this possibility. This is in part because the cleaved peptide bond is located in the flexible D-loop region (residues ~40–50), where the electron density is not normally observed even in intact actin structures. The remaining polypeptide backbone shows variations between the non-equivalent monomers A and B, and between ECP-actin monomers and intact actins in closed conformation. All of these differences are within a range observed among the various crystal structures of complexed actins (Figures 3, 4).

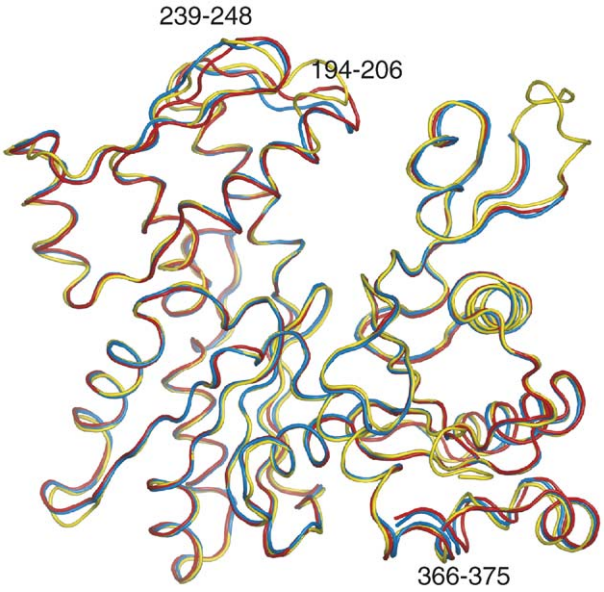

Figure 3. Structure of monomeric ECP-actin. Main-chain structures of ECP-actin monomers A and B (red and blue) are superposed on the structure of intact actin in the complex with DNAse I (yellow). It is clear that the proteolytic cleavage by ECP32 does not significantly affect the overall structure of actin in its monomeric non-polymerized form. The regions where the difference between two ECP-actin molecules is most pronounced are labeled by residue numbers.

In order to draw comparisons among ECP-actin monomers and to the existing structures of intact complexed actins, and to make the comparison visually intuitive, the Mplot procedure was used.[52] In it, pairwise distances between mainchain alpha carbons of the superposed molecules are mapped to a gray scale. Figure 4 shows the Mplot comparison between two non-crystallographically related ECP-actin monomers and a number of representative crystal structures of complexed actins. The graph further emphasizes that the observed ECP-actins are not in any way anomalous when compared to actin in various representative complexes – for every specific difference between ECP-actin and a particular actin complex, another actin complex that does not show such difference can be found. In addition, the Mplot makes clear that the main differences between the ECP-actin monomers A and B, as well as differences between ECP-actin and complexed actins, cluster to a few restricted parts of the molecule. In addition to the D-loop, a region that is so flexible that it is not commonly observed in the crystal structures, this includes another part of the subdomain 2, residues ~55–68. In actin subdomain 4, most variable regions are located in two stretches of residues, ~195–205 and ~232–246. Lastly, both of the actin termini, located in subdomain 1, are conformationally flexible: the N-terminus (residues 1-4), which is rarely observed in the X-ray structures, and a broad C-terminal region, where residues ~350–375 display increased variation, with the

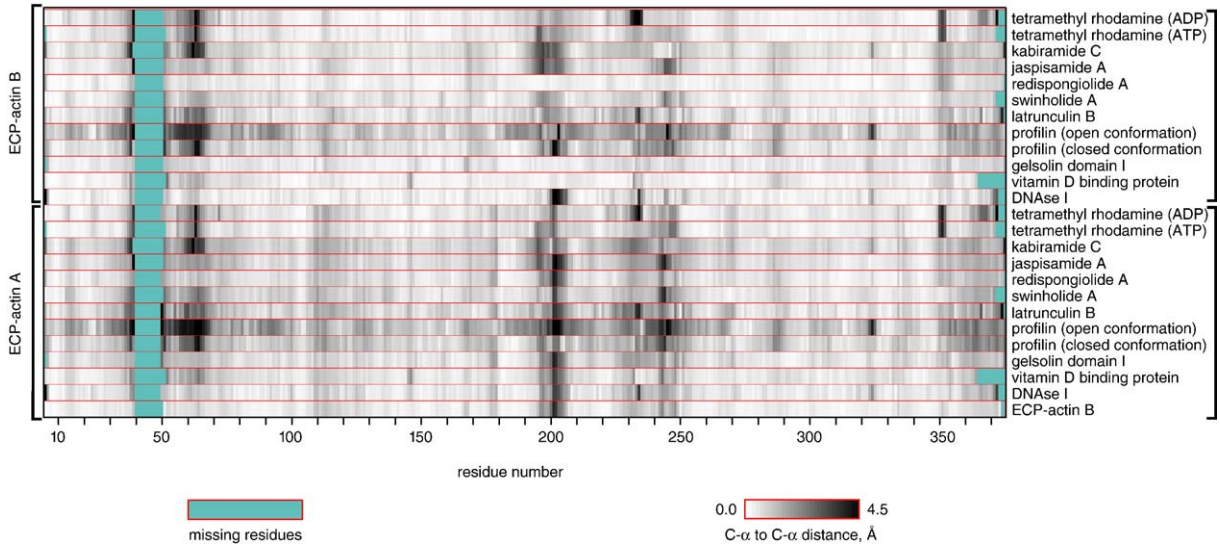

Figure 4. Structural variability in ECP-actin and in intact complexed actin structures. Structures of intact actin in representative complexes (labeled at right) were aligned to the ECP-actin monomer A (lower section) or monomer B (upper section) to find the best fit for the least flexible actin "core" region.[10] Subsequently, the pairwise distances between main chain C^{α} atoms for each matching residue were mapped to a grey scale value to visualize the differences between each pair of the aligned structures.[52] The darker areas correspond to greater distances and reveal "hotspots" of intrinsically flexible actin regions.

most terminal residues frequently disordered and absent in the crystal structures. Perhaps not surprisingly, these "hotspots" of actin structural variability also have higher B-factors values in the crystal structures, which is indicative of their higher conformational flexibility. It is certainly not a coincidence that many of these most variable and flexible regions (the D-loop, the "195–205 loop", C-terminus) represent actin-specific inserts into an ancient actin fold[20] and they are believed, based on existing F-actin models[11,12,43,44] to be involved in the actin-actin contacts in the polymer. Taken together, these observations reinforce the notion that actin polymerization predominantly involves rearrangements of these flexible regions rather than global conformational changes in the molecule.[10]

What does crystal structure of actin represent?

Two conclusions can be immediately drawn from the ECP-actin crystal structure. First, it is now clear that sequestration of actin by actin binding proteins, toxins or its chemical modification by tetramethylrhodamine does not substantially alter its overall structure as seen in crystal structures. Second, the inevitable inference seems to be that crystallization preferentially traps actin in only one of its possible conformations. Indeed, ECP-actin was deduced to have a much more open conformation in solution.[15,49] This is in contrast with the majority of actin complexes in which the binding partners shift the equilibrium toward a more closed conformation, as evidenced by the decrease in the nucleotide exchange rates.[14,40–42] And yet, their crystal structures are so remarkably similar. The energy difference between open and closed states may be sufficiently small that the changes in water activity required for crystallization or differences in crystal packing may shift the equilibrium to one state.[53,54] What, then, do the observed crystal structures represent relative to actin's conformation(s) in solution and in F-actin filaments? A number of possibilities may be considered.

Theoretically, it is possible that the observed actin crystal structures represent the true structure of monomeric G-actin. After all, in all cases the crystal structures have been obtained for actins that either have been rendered polymerization-deficient (actin complexes) or do not polymerize under crystallization conditions (ECP-actin), i.e. for actin monomers. The only data that at present directly contradicts this conclusion comes from a small angle neutron scattering study that suggests that the structure of G-actin is best described as a sphere that is quite different from the oblate ellipsoid seen in crystal structures.[22] The alternative view is that the crystal structures of actin are more closely related to actin structure in its polymeric form. This is certainly consistent with the fact that very successful electron microscopy reconstructions of F-actin require only minor alterations of actin crystal structures.[19,21,44,55,56] Small angle neutron scattering by F-actin is also in good agreement with this conclusion.[22] Additionally, it should be noted that, without exception, all actin crystals have been grown under salt conditions permissive to actin polymerization. If the salt-dependent structural rearrangements in actin do not require actin-actin interaction, the salt present in the crystallization medium should be sufficient to convert the molecule into an F-actin like state.

With regard to the structural identities of the closed and open conformations, crystal structures have thus

far produced limited insights. If the G-actin structure does indeed closely match the structure in actin crystals, then the closed conformation in solution almost certainly corresponds to that seen in typical crystal structures. For the open conformation, the best candidate is a unique conformation observed in one form of actin-profilin crystals,[37] consistent with enhancement of nucleotide exchange in solution.[13,57] Such an interpretation is corroborated by a compelling analysis of the domain movements in actin[10] that indicates that opening of the nucleotide binding cleft is mediated by coordinated movements in the "shear" region between actin subdomains 1 and 3, as well as the similar domain motions observed in distant actin homologs.[5–8] Nevertheless, the relevance of the profilin-bound open conformation to the putative open conformation of actin is not entirely conclusive. A recent molecular dynamics simulation study suggests an inherent instability of this open form in the absence of bound profilin.[39] Another conformational transition that could underlie opening of the nucleotide cleft is the proposed rotation of subdomain 2 around a hinge in its base.[10] In support of this possibility, it has been found that the accessibility of residues 61-68 in the subdomain to limited proteolysis is strongly inhibited by physiological salt concentration in both G- and F-actin.[58,59] Indirectly, this idea is also supported by the fact that the residues 55-68 of the cleft-forming region of actin subdomain 2 display much greater conformational flexibility than the most of the rest of the molecule (Figure 5) but no supporting X-ray structure has yet been reported.

The absence of a clear structural explanation for the significant structural changes detected in ECP-actin by biochemical methods is reminiscent of two similar cases involving actin crystal structures. ADP-actin apparently exhibits a more open conformation than the ATP-bound form[15,19,21] and such an open conformation was observed in crystal structures of Arp3, a close homolog of actin.[60] Yet, in the available crystal structures of ADP-actin, the nucleotide binding cleft remains closed.[23,25] Another example concerns the specific effects of divalent metal ions. The average conformation of Mg^{2+}-ATP-actin in solution is clearly more closed in comparison to the Ca^{2+}-ATP-actin[15,17,61] and it polymerizes much better.[51,61,62] Nevertheless, a systematic comparison between structures with Ca^{2+} and Mg^{2+} tightly bound with ATP in the nucleotide binding cleft does not reveal any obvious metal-specific tertiary structure differences despite clear differences in metal coordination number[31] (also V.K. and I.R., unpublished).

Nature of low affinity divalent cation binding sites

In addition to the strongly bound divalent cation chelated by protein and nucleotide, actin properties and conformational dynamics are further influenced by divalent metal ions binding to a number of low affinity sites. The function of the low affinity sites is attributed to stabilization of actin nuclei, thereby increasing the overall polymerization rate, and/or

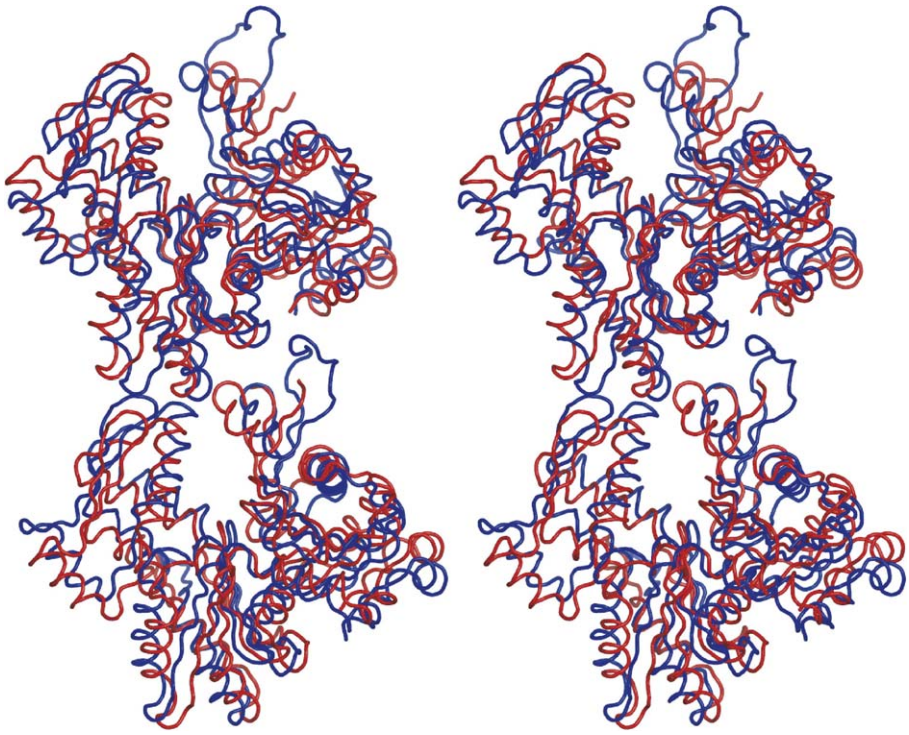

Figure 5. Stereo figure of F-actin-like longitudinal actin dimer in the ECP-actin crystal lattice. Shown in red is an F-actin-like dimer formed by monomer B and monomer A from a symmetry-related antiparallel dimer. Shown in blue is the same dimer from the F-actin model[43] superposed onto the ECP-actin dimer. The pairwise r.m.s.d. between the two structures is 4.0 Å for all matching C^{α} atoms.

"monomer activation" that results in enhanced nucleation.[61,62] The identity of these low affinity sites, however, is unknown. In the ECP-actin structure, three strontium ions are bound at secondary binding sites (Figure 2(a)). In monomer A, a Sr^{2+} ion interacts *via* bridging water molecules with Asp222, Glu224 and Glu316; in monomer B, Sr^{2+} is coordinated by the carbonyl oxygen of Val30 and is held there by bridging waters ultimately connecting it to Asp56 and Glu93, and in both monomers Sr^{2+} ions are positioned between Glu125 and Asn128. None of these sites are specific to strontium because the same sites are also occupied in the structure obtained from less well diffracting but otherwise identical Ca^{2+}-ECP-actin crystals (data not shown).

Although in crystal structures the observed secondary metal binding sites are not necessarily physiologically relevant, some of the physiological sites are expected to be occupied. The observation that two of the binding sites found in ECP-actin are very similar to those observed for Ca^{2+} in ADP-actin modified with tetramethyl-rhodamine prompted an analysis of coordinated secondary metal ions in all available actin structures. The results are summarized in Table 2. It shows that while there are some subtle differences in the details of coordination, of the seven sites reported to date four have been observed in multiple crystal structures. It seems extremely unlikely that identical metal binding sites would be preserved as an artifact of crystallization conditions across a wide range of crystal lattices, types and concentrations of divalent ions, and pH values ranging from 5.0 to 8.5. Therefore, sites 1 through 4 listed in Table 2 are most likely to be physiologically relevant and are expected to be occupied by Mg^{2+} under intracellular conditions. Since actin mutants can now be expressed on a large scale using a baculovirus expression system,[63] mutagenic studies promise to be instrumental in delineating the functional importance of each of the identified low affinity cation binding sites.

Table 2. Secondary metal-binding sites observed in crystal structures of actin

Site	Cation	Coordinating residues	PDB code and references
1	Ca^{2+}	D222, E224	1J6Z[25], 2FXU[36]
	Sr^{2+}	D222-W[a], E224-W, E316-W	This study
	Cd^{2+}	D222	1P8Z[29]
2	Ca^{2+}	Q263, S265, E270-W, S271-W	2FXU[36]
	Ca^{2+}	Q263, S265, S271-W, M269-W	2ASM[33], 2A5X[35]
	Ca^{2+}	E270, G286	1J6Z[25]
3	Ca^{2+}	E205, S199-W	1J6Z[25]
	Mg^{2+}	E205, S199-W	1YXQ[34]
4	Ca^{2+}	V30, E93-W	1J6Z[25]
	Sr^{2+}	V30, E93-W, D56-W	This study
5	Ca^{2+}	Q354, Q354-W, W356, E361	1J6Z[25], 1NWK[28]
6	Ca^{2+}	D286, D288	1NWK[28], 2FXU[36]
7	Sr^{2+}	E125, N128	This study

[a] "W" next to the residue indicates that the interaction is mediated through a bridging water molecule.

Nature of actin-actin contacts in F-actin

There is now widespread consensus that the F-actin models correctly establish the overall topological arrangement of actin subunits in the filament. Still, the high resolution information needed to establish precise nature of actin-actin contacts is not yet available. The seductive appeal of extracting some of this information from crystal structures is very strong. The ECP-actin structure provides an example of symmetry-related actin-actin contacts that strongly resemble the longitudinal actin dimer predicted by the existing F-actin models (Figure 5). As such, ECP-actin joins a series of recent structures of complexed actins that display similar, though not identical, contacts between crystallographic symmetry-related neighbors: Latrunculin A-bound cross-linked actin dimer,[35] actin-sphinxolide B complex,[33] and actin-bistramide A complex.[36] The distance between the centers of mass in the longitudinal ECP-actin dimer is identical to that in F-actin, 55 Å. Essentially the same distance was also found for the complexed actin dimers formed by pure translation along the cell axis –54.4, 55, 56.5 Å for cross-linked latrunculin-bound dimer, actin- sphinxolide B and actin-bistramide A, respectively. Taking into account the significant differences in crystal cell dimensions, crystal packing and crystallization conditions, this is certainly not a coincidence. These structures correspond either to uncomplexed ECP-actin or to actin in complex with small organic ligands – a fact that enables actin molecules to come into close apposition in what is likely to be an energetically favorable arrangement. Accordingly, in the case of the cross-linked actin dimer structure it has been strongly argued that the interaction between subdomain 4 and subdomain 3 observed in the crystal suggests the true molecular interface between neighbor protomers in F-actin,[35] even though the molecules in the crystal are related by pure translation and lack F-actin's helical twist. There are two unique features of ECP-actin structure: First, the dimer is formed by two crystallographically independent molecules of actin and second is that, unlike in others, the F-actin-like twist is present. In ECP-actin dimer the monomers are rotated in relation to each other by ~20° – in comparison to the 28° twist in the most typical actin filaments. The similarity of the ECP-actin symmetry-related dimer and longitudinal dimer of the original Holmes model[43] is significant enough to allow a compelling superposition that gives an r.m.s.d. of only 4.0 Å over all backbone Cα atoms (Figure 5). A structural alignment with the recent refined F-actin model,[44] however, is not as good, yielding an r.m.s.d. of 5.6 Å. This is likely caused by the fact that the recent refined model is significantly distorted over entire protein backbone and does not align well even with individual ECP-actin monomers (r.m.s.d. values are 4.1 and 4.3 Å for the ECP-actin upper and lower monomers, respectively; this is to be contrasted with the 1.2 Å r.m.s.d. when either of the ECP-actin monomers are superposed onto original Holmes model that is based on actin-DNAse crystal structure).

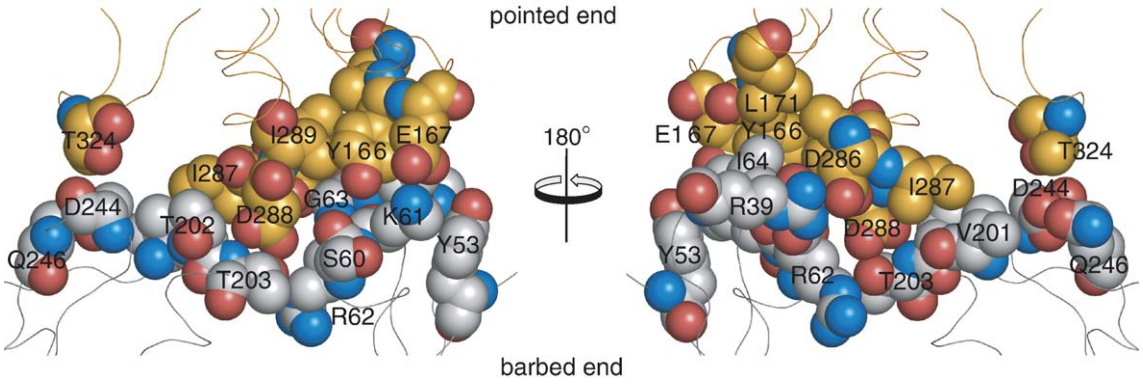

Figure 6. Molecular interface of the F-actin-like contacts in the ECP-actin crystal lattice. Residues comprising the molecular interface are shown as spacefill representations with carbon atoms colored as gray and orange for the different actin molecules. Oxygen atoms are red and nitrogen atoms are blue.

A detailed molecular interface in the longitudinal ECP-actin dimer is presented in Figure 6. The total solvent-accessible surface area buried on this interface is 669 Å^2. This is surprisingly similar to the interface between crystallographically-related actins where the monomers are not rotated against each other: 656 Å^2 for actin-sphinxolide B, 718 Å^2 for bistramide A, and 550 Å^2 for the latrunculin bound cross-linked actin dimer. The slightly different total buried areas indicate that at least some specific actin-actin interactions must differ. The question then arises – are any of the experimentally observed contacts physiological and if yes, which ones? It should be noted that F-actin filaments exhibit a high degree of rotational freedom such that the helical twist can deviate ±10–12° from the ideal geometry present in F-actin models.[55,64,65] It seems therefore likely that many of the observed interactions can be indeed "real" and that the most prudent approach is to pay close attention to all of them. To this end, Table 3 summarizes the putative F-actin-like contacts observed in the crystal structures to date. Following the convincing argument presented for the cross-linked actin dimer,[35] there is absolutely no doubt that a plausible F-actin model that incorporates most of the experimentally observed features of actin-actin interfaces can be built. In the absence of a high resolution F-actin structure, the specific actin-actin contacts observed in actin crystal structures are the best candidates for mutagenic studies that will help to delineate the true actin-actin interfaces in the actin filaments.

Materials and Methods

Actin purification, preparation of ECP actin

Actin was purified from rabbit muscle acetone powder by extraction with 0.4 M ammonium thiocyanate followed by chromatography on hydroxyapatite in the presence of 0.2 M ammonium thiocyanate and a cycle of polymerization and depolymerization (D. Smith, R.W. Smith, I.R., unpublished; described in supplemental materials by Allingham *et al.*[33]). For the proteolytic cleavage, actin in G-buffer (2 mM Tris, 0.2 mM ATP, 0.2 mM $CaCl_2$, 1 mM NaN_3, 1 mM TCEP, pH 8.0) was incubated for two hours at room temperature with an optimal amount of purified ECP32 preparation,[46] concentrated by ultrafiltration to 10-

Table 3. F-actin-like interactions observed in actin crystal structures

Close contacts (lower-upper monomer)	ECP-actin, this work	Actin with bistramide A, 2FXU[36]	Cross-linked actin dimer, 2A5X[35]	Actin with sphinxolide B, 2ASO[33]
Salt bridges, 3.5 Å				
Arg39-Asp286	Yes	Yes		
Lys61-Glu167	Yes	Yes		
Glu205-Lys291			Yes	Yes
H-bonds, 3.5 Å				
Thr203-Asp288	Yes	Yes	Yes	Yes
Ser199-Lys291			Yes	Yes
Gln246-Thr324		Yes		
Hydrophobic, 4 Å				
Gln41-Leu171		Yes		
Gly63-Asp286	Yes			
Gly63-Tyr166				Yes
Ile64-Tyr166	Yes	Yes		
Ile64-Glu167				Yes
Val201-Ile287	Yes	Yes	Yes	
Thr202-Lys291			Yes	
Val203-Asp288	Yes			Yes

15 mg/ml, frozen in liquid nitrogen and stored at −80 °C. Optimal actin/ECP32 ratio was determined empirically for each batch of purified actin and protease.

Crystallization and cryopreservation

Initial ECP-actin crystals were obtained in a sparse matrix screen after streak seeding with crystals of jaspisamide A-ECP-actin complex, which grew spontaneously under the same conditions as crystals of non-modified actin complexed to jaspisamide A.[30] The largest and the best diffracting ECP-actin crystals were grown at 4 °C by microseeding 10 μl hanging drops as a 1:1 mixture of 5–7.5 mg/ml protein (in G-buffer with an additional 0.5 mM ATP added) and precipitant solution (40 mM $SrCl_2$, 10% ethylene glycol, 13–15% dimethyl polyethylene glycol 5000, 50 mM triethanolamine, 10 mM spermidine, pH 7.75) equilibrated against 0.5 ml precipitant. Very thin plates grew in clusters in three to four days. The crystals were unstable: the diffraction limit decayed rapidly within a week and the crystals themselves tended to disintegrate within a month. Identical crystals were also grown in the presence of $CaCl_2$ in place of $SrCl_2$ but they did not diffract as strongly. Ethylene glycol was essential for the crystal growth and stability while the inclusion of spermidine was found to increase diffraction limit by about 0.5 Å. Crystals were cryopreserved by transfer into the precipitant solution followed by three equal steps of increasing concentrations of ethylene glycol and polyethylene glycol 5000 (to the 20% and 25% final, respectively) and flash frozen in a stream of cold liquid nitrogen gas.

Data processing, structure solution and refinement

Data were collected at the 19-BM beamline of the Structural Biology Center at the Advanced Photon Source in Argonne, IL as two datasets of 478 frames each of width 0.5° at wavelength of 0.9184 Å. Diffraction data were integrated and scaled with HKL2000.[66] The structure was solved by molecular replacement with Phaser[67] using two copies of the model (PDB accession code **1J6Z**[25]) in the asymmetric unit cell. The structure was refined with Refmac.[68] Water molecules were added to the coordinate set with ARP/wARP[69] with subsequent manual verification. Figures were prepared with Pymol†.

Protein Data Bank accession code

The coordinates and structure factors have been deposited in the RCSB Protein Data Bank under accession code 2HMP.

Acknowledgements

We are grateful to Dr. Alevtina Morozova for providing us with protease ECP 32 and to Dr. Junichi Tanaka for his generous gift of halichondramide. We thank Dr. Martin St Maurice for critical reading of the manuscript. The work was supported by National Institutes of Health grant AR35186 to I. R. and by Russian Foundation for Basic Research grant 05-04-49604 to S.K.

† http://www.pymol.org

References

1. Pollard, T. D., Blanchoin, L. & Mullins, R. D. (2000). Molecular mechanisms controlling actin filament dynamics in nonmuscle cells. *Annu. Rev. Biophys. Biomol. Struct.* **29**, 545–576.
2. Kabsch, W. & Holmes, K. C. (1995). The actin fold. *Faseb J.* **9**, 167–174.
3. Hurley, J. H. (1996). The sugar kinase/heat shock protein 70/actin superfamily: implications of conserved structure for mechanism. *Annu. Rev. Biophys. Biomol. Struct.* **25**, 137–162.
4. Egelman, E. H. (2003). Actin's prokaryotic homologs. *Curr. Opin. Struct. Biol.* **13**, 244–248.
5. Bennett, W. S., Jr & Steitz, T. A. (1980). Structure of a complex between yeast hexokinase A and glucose: II. Detailed comparisons of conformation and active site configuration with the native hexokinase B monomer and dimer. *J. Mol. Biol.* **140**, 211–230.
6. Steitz, T. A., Shoham, M. & Bennett, W. S., Jr (1981). Structural dynamics of yeast hexokinase during catalysis. *Philos. Trans. R. Soc. Lond. B. Biol. Sci.* **293**, 43–52.
7. Zhang, Y. & Zuiderweg, E. R. (2004). The 70-kDa heat shock protein chaperone nucleotide-binding domain in solution unveiled as a molecular machine that can reorient its functional subdomains. *Proc. Natl Acad. Sci. USA*, **101**, 10272–10277.
8. Mayer, M. P. & Bukau, B. (2005). Hsp70 chaperones: cellular functions and molecular mechanism. *Cell Mol. Life Sci.* **62**, 670–684.
9. Tirion, M. M. & ben-Avraham, D. (1993). Normal mode analysis of G- actin. *J. Mol. Biol.* **230**, 186–195.
10. Page, R., Lindberg, U. & Schutt, C. E. (1998). Domain motions in actin. *J. Mol. Biol.* **280**, 463–474.
11. Lorenz, M., Popp, D. & Holmes, K. C. (1993). Refinement of the F-actin model against X-ray fiber diffraction data by the use of a directed mutation algorithm. *J. Mol. Biol.* **234**, 826–836.
12. Tirion, M. M., ben-Avraham, D., Lorenz, M. & Holmes, K. C. (1995). Normal modes as refinement parameters for the F-actin model. *Biophys. J.* **68**, 5–12.
13. Kinosian, H. J., Selden, L. A., Gershman, L. C. & Estes, J. E. (2000). Interdependence of profilin, cation, and nucleotide binding to vertebrate non-muscle actin. *Biochemistry*, **39**, 13176–13188.
14. Kudryashov, D. S. & Reisler, E. (2003). Solution properties of tetramethylrhodamine-modified G-actin. *Biophys. J.* **85**, 2466–2475.
15. Strzelecka-Golaszewska, H., Moraczewska, J., Khaitlina, S. Y. & Mossakowska, M. (1993). Localization of the tightly bound divalent-cation-dependent and nucleotide-dependent conformation changes in G-actin using limited proteolytic digestion. *Eur. J. Biochem.* **211**, 731–742.
16. Yao, X., Nguyen, V., Wriggers, W. & Rubenstein, P. A. (2002). Regulation of yeast actin behavior by interaction of charged residues across the interdomain cleft. *J. Biol. Chem.* **277**, 22875–22882.
17. Guan, J. Q., Almo, S. C., Reisler, E. & Chance, M. R. (2003). Structural reorganization of proteins revealed by radiolysis and mass spectrometry: G-actin solution

structure is divalent cation dependent. *Biochemistry*, **42**, 11992–12000.
18. Guan, J. Q., Takamoto, K., Almo, S. C., Reisler, E. & Chance, M. R. (2005). Structure and dynamics of the actin filament. *Biochemistry*, **44**, 3166–3175.
19. Belmont, L. D., Orlova, A., Drubin, D. G. & Egelman, E. H. (1999). A change in actin conformation associated with filament instability after Pi release. *Proc. Natl Acad. Sci. USA*, **96**, 29–34.
20. Galkin, V. E., VanLoock, M. S., Orlova, A. & Egelman, E. H. (2002). A new internal mode in F-actin helps explain the remarkable evolutionary conservation of actin's sequence and structure. *Curr. Biol.* **12**, 570–575.
21. Sablin, E. P., Dawson, J. F., VanLoock, M. S., Spudich, J. A., Egelman, E. H. & Fletterick, R. J. (2002). How does ATP hydrolysis control actin's associations? *Proc. Natl Acad. Sci. USA*, **99**, 10945–10947.
22. Norman, A. I., Ivkov, R., Forbes, J. G. & Greer, S. C. (2005). The polymerization of actin: structural changes from small-angle neutron scattering. *J. Chem. Phys.* **123**, 154904.
23. Kabsch, W., Mannherz, H. G., Suck, D., Pai, E. F. & Holmes, K. C. (1990). Atomic structure of the actin: DNase I complex. *Nature*, **347**, 37–44.
24. Schutt, C. E., Myslik, J. C., Rozycki, M. D., Goonesekere, N. C. & Lindberg, U. (1993). The structure of crystalline profilin-beta-actin. *Nature*, **365**, 810–816.
25. Otterbein, L. R., Graceffa, P. & Dominguez, R. (2001). The crystal structure of uncomplexed actin in the ADP state. *Science*, **293**, 708–711.
26. Bubb, M. R., Govindasamy, L., Yarmola, E. G., Vorobiev, S. M., Almo, S. C., Somasundaram, T. *et al.* (2002). Polylysine induces an antiparallel actin dimer that nucleates filament assembly: crystal structure at 3.5-Å resolution. *J. Biol. Chem.* **277**, 20999–21006.
27. Otterbein, L. R., Cosio, C., Graceffa, P. & Dominguez, R. (2002). Crystal structures of the vitamin D-binding protein and its complex with actin: structural basis of the actin-scavenger system. *Proc. Natl Acad. Sci. USA*, **99**, 8003–8008.
28. Graceffa, P. & Dominguez, R. (2003). Crystal structure of monomeric actin in the ATP state. Structural basis of nucleotide-dependent actin dynamics. *J. Biol. Chem.* **278**, 34172–34180.
29. Irobi, E., Burtnick, L. D., Urosev, D., Narayan, K. & Robinson, R. C. (2003). From the first to the second domain of gelsolin: a common path on the surface of actin? *FEBS Lett.* **552**, 86–90.
30. Klenchin, V. A., Allingham, J. S., King, R., Tanaka, J., Marriott, G. & Rayment, I. (2003). Trisoxazole macrolide toxins mimic the binding of actin-capping proteins to actin. *Nat. Struct. Biol.* **10**, 1058–1063.
31. Vorobiev, S., Strokopytov, B., Drubin, D. G., Frieden, C., Ono, S., Condeelis, J. *et al.* (2003). The structure of nonvertebrate actin: implications for the ATP hydrolytic mechanism. *Proc. Natl Acad. Sci. USA*, **100**, 5760–5765.
32. Reutzel, R., Yoshioka, C., Govindasamy, L., Yarmola, E. G., Agbandje-McKenna, M., Bubb, M. R. & McKenna, R. (2004). Actin crystal dynamics: structural implications for F-actin nucleation, polymerization, and branching mediated by the anti-parallel dimer. *J. Struct. Biol.* **146**, 291–301.
33. Allingham, J. S., Zampella, A., D'Auria, M. V. & Rayment, I. (2005). Structures of microfilament destabilizing toxins bound to actin provide insight into toxin design and activity. *Proc. Natl Acad. Sci. USA*, **102**, 14527–14532.
34. Klenchin, V. A., King, R., Tanaka, J., Marriott, G. & Rayment, I. (2005). Structural basis of swinholide A binding to actin. *Chem. Biol.* **12**, 287–291.
35. Kudryashov, D. S., Sawaya, M. R., Adisetiyo, H., Norcross, T., Hegyi, G., Reisler, E. & Yeates, T. O. (2005). The crystal structure of a cross-linked actin dimer suggests a detailed molecular interface in F-actin. *Proc. Natl Acad. Sci. USA*, **102**, 13105–13110.
36. Rizvi, S. A., Tereshko, V., Kossiakoff, A. A. & Kozmin, S. A. (2006). Structure of bistramide a-actin complex at a 1.35 Å resolution. *J. Am. Chem. Soc.* **128**, 3882–3883.
37. Chik, J. K., Lindberg, U. & Schutt, C. E. (1996). The structure of an open state of beta-actin at 2.65 Å resolution. *J. Mol. Biol.* **263**, 607–623.
38. Dominguez, R. & Graceffa, P. (2003). Solution properties of TMR-actin: when biochemical and crystal data agree. *Biophys. J.* **85**, 2073–2074.
39. Minehardt, T. J., Kollman, P. A., Cooke, R. & Pate, E. (2006). The open nucleotide pocket of the profilin/actin x-ray structure is unstable and closes in the absence of profilin. *Biophys. J.* **90**, 2445–2449.
40. Saito, S., Watabe, S., Ozaki, H., Kigoshi, H., Yamada, K., Fusetani, N. & Karaki, H. (1996). Novel actin depolymerizing macrolide aplyronine A. *J. Biochem. (Tokyo)*, **120**, 552–555.
41. Yarmola, E. G., Somasundaram, T., Boring, T. A., Spector, I. & Bubb, M. R. (2000). Actin-latrunculin A structure and function. Differential modulation of actin-binding protein function by latrunculin A. *J. Biol. Chem.* **275**, 28120–28127.
42. Dawson, J. F., Sablin, E. P., Spudich, J. A. & Fletterick, R. J. (2003). Structure of an F-actin trimer disrupted by gelsolin and implications for the mechanism of severing. *J. Biol. Chem.* **278**, 1229–1238.
43. Holmes, K. C., Popp, D., Gebhard, W. & Kabsch, W. (1990). Atomic model of the actin filament. *Nature*, **347**, 44–49.
44. Holmes, K. C., Schroder, R. R., Sweeney, H. L. & Houdusse, A. (2004). The structure of the rigor complex and its implications for the power stroke. *Philos. Trans. R. Soc. Lond. B. Biol. Sci.* **359**, 1819–1828.
45. Khaitlina, S., Collins, J. H., Kuznetsova, I. M., Pershina, V. P., Synakevich, I. G., Turoverov, K. K. & Usmanova, A. M. (1991). Physico-chemical properties of actin cleaved with bacterial protease from E. coli A2 strain. *FEBS Lett.* **279**, 49–51.
46. Matveyev, V. V., Usmanova, A. M., Morozova, A. V., Collins, J. H. & Khaitlina, S. Y. (1996). Purification and characterization of the proteinase ECP 32 from Escherichia coli A2 strain. *Biochim. Biophys. Acta*, **1296**, 55–62.
47. Khaitlina, S. Y., Moraczewska, J. & Strzelecka-Golaszewska, H. (1993). The actin/actin interactions involving the N-terminus of the DNase-I-binding loop are crucial for stabilization of the actin filament. *Eur. J. Biochem.* **218**, 911–920.
48. Wawro, B., Khaitlina, S. Y., Galinska-Rakoczy, A. & Strzelecka-Golaszewska, H. (2005). Role of actin DNase-I-binding loop in myosin subfragment 1-induced polymerization of G-actin: implications for the mechanism of polymerization. *Biophys. J.* **88**, 2883–2896.
49. Khaitlina, S. Y. & Strzelecka-Golaszewska, H. (2002). Role of the DNase-I-binding loop in dynamic properties of actin filament. *Biophys. J.* **82**, 321–334.
50. Steinmetz, M. O., Goldie, K. N. & Aebi, U. (1997). A correlative analysis of actin filament assembly, structure, and dynamics. *J. Cell Biol.* **138**, 559–574.

51. Steinmetz, M. O., Stoffler, D., Hoenger, A., Bremer, A. & Aebi, U. (1997). Actin: from cell biology to atomic detail. *J. Struct. Biol.* **119**, 295–320.
52. Alwyn Jones, T. & Kleywegt, G. J. (1999). CASP3 comparative modeling evaluation. *Proteins*, **Suppl. 3**, 30–46.
53. Gerstein, M., Lesk, A. M. & Chothia, C. (1994). Structural mechanisms for domain movements in proteins. *Biochemistry*, **33**, 6739–6749.
54. Simanshu, D. K., Savithri, H. S. & Murthy, M. R. (2005). Crystal structures of ADP and AMPPNP-bound propionate kinase (TdcD) from Salmonella typhimurium: comparison with members of acetate and sugar kinase/heat shock cognate 70/actin superfamily. *J. Mol. Biol.* **352**, 876–892.
55. Galkin, V. E., Orlova, A., Koleske, A. J. & Egelman, E. H. (2005). The Arg non-receptor tyrosine kinase modifies F-actin structure. *J. Mol. Biol.* **346**, 565–575.
56. Volkmann, N., Liu, H., Hazelwood, L., Krementsova, E. B., Lowey, S., Trybus, K. M. & Hanein, D. (2005). The structural basis of myosin V processive movement as revealed by electron cryomicroscopy. *Mol. Cell*, **19**, 595–605.
57. Blanchoin, L. & Pollard, T. D. (1998). Interaction of actin monomers with Acanthamoeba actophorin (ADF/cofilin) and profilin. *J. Biol. Chem.* **273**, 25106–25111.
58. Khaitlina, S., Wawro, B., Pliszka, B. & Strzelecka-Golaszewska, H. (1996). Conformational changes associated with the monomer activation step of actin polymerization. *J. Muscle Res. Cell Motil*, **16**, 122–123.
59. Strzelecka-Golaszewska, H., Wozniak, A., Hult, T. & Lindberg, U. (1996). Effects of the type of divalent cation, Ca^{2+} or Mg^{2+}, bound at the high-affinity site and of the ionic composition of the solution on the structure of F-actin. *Biochem. J.* **316**, 713–721.
60. Nolen, B. J., Littlefield, R. S. & Pollard, T. D. (2004). Crystal structures of actin-related protein 2/3 complex with bound ATP or ADP. *Proc. Natl Acad. Sci. USA*, **101**, 15627–15632.
61. Strzelecka-Golaszewska, H. (2001). Divalent cations, nucleotides, and actin structure. *Results Probl. Cell Differ.* **32**, 23–41.
62. Estes, J. E., Selden, L. A., Kinosian, H. J. & Gershman, L. C. (1992). Tightly-bound divalent cation of actin. *J. Muscle Res. Cell Motil.* **13**, 272–284.
63. Joel, P. B., Fagnant, P. M. & Trybus, K. M. (2004). Expression of a nonpolymerizable actin mutant in Sf9 cells. *Biochemistry*, **43**, 11554–11559.
64. Egelman, E. H., Francis, N. & DeRosier, D. J. (1982). F-actin is a helix with a random variable twist. *Nature*, **298**, 131–135.
65. Schmid, M. F., Sherman, M. B., Matsudaira, P. & Chiu, W. (2004). Structure of the acrosomal bundle. *Nature*, **431**, 104–107.
66. Otwinowski, Z. & Minor, W. (1997). Processing of X-ray diffraction data collected in oscillation mode. *Methods in Enzymology*, **276**, 307–326.
67. Storoni, L. C., McCoy, A. J. & Read, R. J. (2004). Likelihood-enhanced fast rotation functions. *Acta Crystallogr. D. Biol. Crystallogr.* **60**, 432–438.
68. Murshudov, G. N., Vagin, A. A. & Dodson, E. J. (1997). Refinement of macromolecular structures by the maximum-likelihood method. *Acta Crystallogr. D. Biol. Crystallogr.* **53**, 240–255.
69. Perrakis, A., Harkiolaki, M., Wilson, K. S. & Lamzin, V. S. (2001). ARP/wARP and molecular replacement. *Acta Crystallogr. D. Biol. Crystallogr.* **57**, 1445–1450.

Edited by R. Huber

(Received 28 April 2006; received in revised form 3 July 2006; accepted 6 July 2006)
Available online 7 August 2006